Combined Internal and External Category-Specific Image Denoising

Saeed Anwar
Saeed.Anwar@anu.edu.au
Cong Phuoc Huynh
Cong.Huynh@anu.edu.au
Fatih Porikli
Fatih.Porikli@anu.edu.au
The Australian National University, Canberra, Australia

In supplementary section of the paper, first we show qualitative and quantitative results for Multiview dataset [5] and then show more qualitative results on the mentioned datasets in the main paper.

1 Multi-view images

Further, we demonstrate the ability of our algorithm in denoising an image given the noise-free images of a similar scene captured in other views. This scenario emerges when one of the multi-view images is corrupted by sensor noise while the other are still noise-free.

For a fair comparison to related methods such as those in [6] and [9], we use ten scenes from Middlebury Computer Vision [5], each scene captured in six views. First view is used as a test image while remaining views are used as training images.

Figure 1 shows the PSNR of our method against the competing methods. Our algorithm is the best performer followed by TID [6]. For high noise variance, the performance of TID [6] degrades and is similar to internal image denoising while our method consistently outperforms both internal denoising and TID. Our average PSNR gain is 0.97 dB over TID and 1.97 dB over EPLL [10] for $\sigma_n = 80$. In figure 2, we demonstrate the visual quality of our method and other denoising algorithms on an image of dolls. When closely examining the textured areas on dolls, we observe that our method recovers finer details and significantly reduces the noise, therefore, yielding higher PSNR. On the other hand, the competing methods either smooths out the texture or creates artifacts on the dolls.

2 More Examples

First, we show the results for low noise levels, $\sigma_n = 10$ and $\sigma_n = 20$ in figures 3 and 4, respectively. Similarly, we present denoising result on building images from dataset [9] in figures 5 and 6.

In figures 7 and 9, we show further results for face images in the Gore dataset [7]. The images restored by our method appear to be more face-like than those achieved by the others, thanks to the category-specific support patches. The proposed algorithm is able to recover

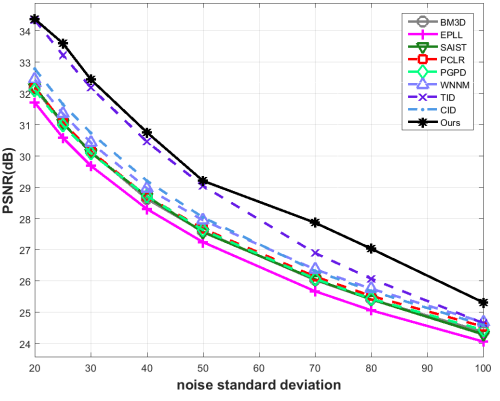

Figure 1: Multiview image denoising: Each PSNR value is averaged over 10 test images with a size of 450×375.

Input	BM3D [7]	PCLR [1]	PGPD [8]	WNNM [4]	TID [6]	Ours
10.07 dB	24.35 dB	24.48 dB	24.39 dB	24.37 dB	24.97 dB	**26.44** dB

Figure 2: Comparison of denoising methods on an image from the Middlebury Computer Vision dataset [5], for $\sigma_n = 80$. Our method is able to recover texture on the dolls while others fail to achieve that.

the weak textures around the eyes and mouth, while state-of-the-art methods fail to recover any textures near the eyes, mouth or nose.

Figures 8 and 10 demonstrate a qualitative comparison with state of the art alternatives for images from the Multiview dataset in [5]. Our proposed method recovers all of the fine details and textures while the others methods produce smoother images with much less details. Overall, our method is robust and achieves higher-quality results than the others.

Figure 3: Denoising sample results (with PSNR) from the Multiview dataset [5] for the noise standard deviation $\sigma_n = 10$.

Figure 4: Denoising results on a bike image [3], for $\sigma_n = 20$. Our method is able to recover sharp boundaries around the bike.

Figure 5: Denoising results on a dataset from [9], for $\sigma_n = 50$. Differences can be better viewed in high resolution.

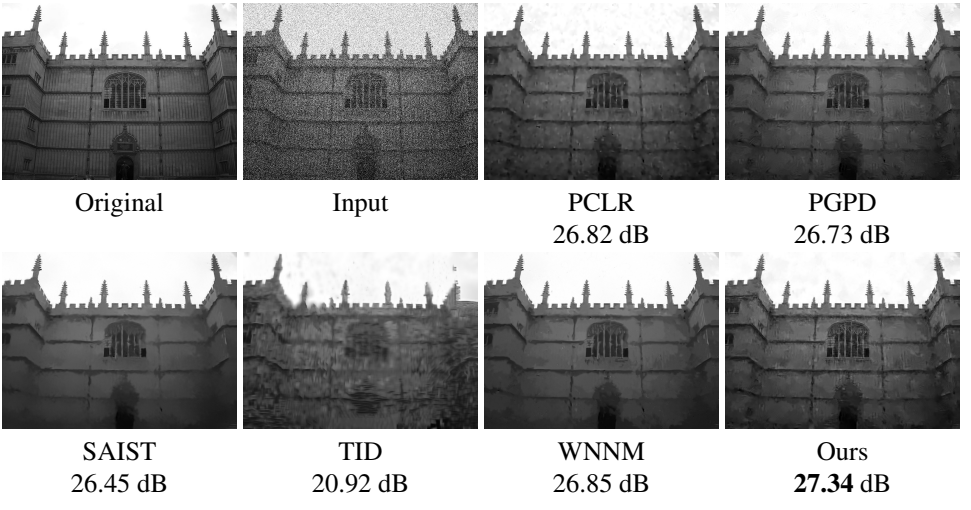

Figure 6: Denoising results on a image from dataset [9], for $\sigma_n = 90$.

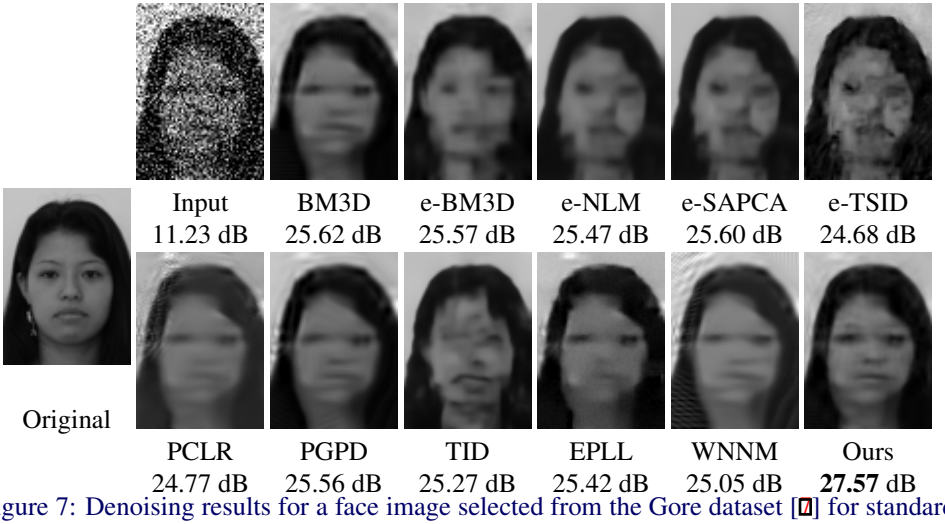

Figure 7: Denoising results for a face image selected from the Gore dataset [7] for standard deviation $\sigma_n = 70$. Differences are better observed in a magnified view.

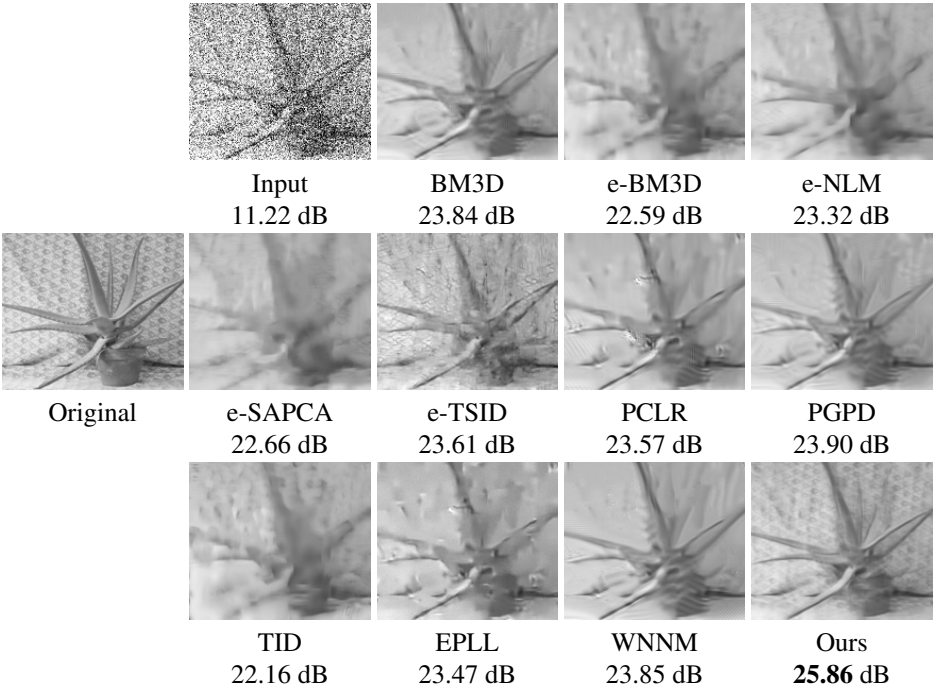

Figure 8: Denoising results (with PSNR) for an image from the Multiview dataset [5] for standard deviation $\sigma_n = 70$.

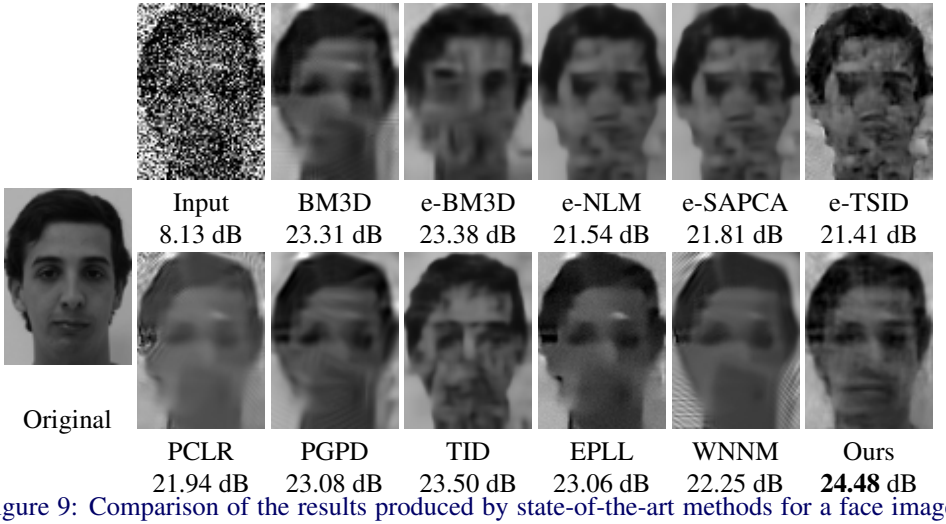

Figure 9: Comparison of the results produced by state-of-the-art methods for a face image selected from the Gore dataset [7] when $\sigma_n = 100$.

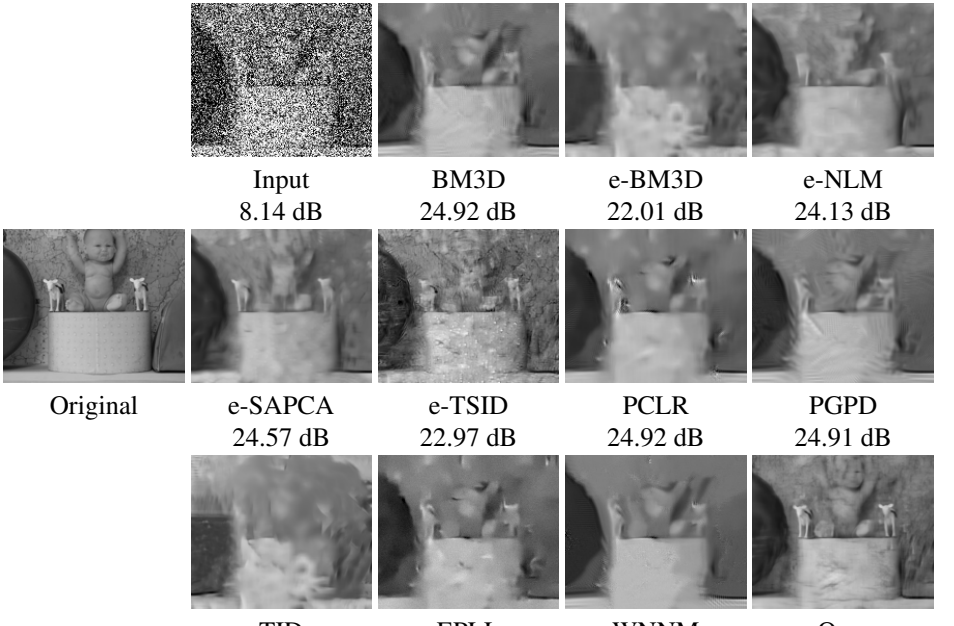

Figure 10: Denoising sample results (with PSNR) from the Multiview dataset [5] for the noise standard deviation $\sigma_n = 100$.

References

[1] Fei Chen, Lei Zhang, and Huimin Yu. External patch prior guided internal clustering for image denoising. 2015.

[2] Kostadin Dabov, Alessandro Foi, Vladimir Katkovnik, and Karen Egiazarian. Image denoising by sparse 3-D transform-domain collaborative filtering. *Image Processing, IEEE Transactions on*, pages 2080–2095, 2007.

[3] Robert Fergus, Pietro Perona, and Andrew Zisserman. Object class recognition by unsupervised scale-invariant learning. In *Computer Vision and Pattern Recognition, 2003. Proceedings. 2003 IEEE Computer Society Conference on*, volume 2, pages II–264. IEEE, 2003.

[4] Shuhang Gu, Lei Zhang, Wangmeng Zuo, and Xiangchu Feng. Weighted nuclear norm minimization with application to image denoising. In *CVPR*, pages 2862–2869, 2014.

[5] Heiko Hirschmüller and Daniel Scharstein. Evaluation of cost functions for stereo matching. In *CVPR*, pages 1–8, 2007.

[6] Enming Luo, Stanley H Chan, and Truong Q Nguyen. Adaptive image denoising by targeted databases. *Image Processing, IEEE Transactions on*, pages 2167–2181, 2015.

[7] Yigang Peng, Arvind Ganesh, John Wright, Wenli Xu, and Yi Ma. Rasl: Robust alignment by sparse and low-rank decomposition for linearly correlated images. *TPAMI*, pages 2233–2246, 2012.

[8] L Xu, L Zhang, W Zuo, D Zhang, and X Feng. Patch group based nonlocal self-similarity prior learning for image denoising. 2015.

[9] H. Yue, X. Sun, J. Yang, and F. Wu. Cid: Combined image denoising in spatial and frequency domains using web images. In *CVPR*, pages 2933–2940, June 2014.

[10] Daniel Zoran and Yair Weiss. From learning models of natural image patches to whole image restoration. In *ICCV*, pages 479–486, 2011.